Adsorption of ammonium on clinoptilolite in presence of competing cations: Investigation on groundwater remediation

Marco Vocciante [a, *], Alessandra De Folly D'Auris [b], Antonio Finocchi [b], Marco Tagliabue [b], Michela Bellettato [c], Aurelio Ferrucci [a], Andrea P. Reverberi [a], Sergio Ferro [d, 1]

[a] Università degli Studi di Genova, Dipartimento di Chimica e Chimica Industriale, Via Dodecaneso 31, 16146 Genova, Italy
[b] Eni S.p.A., Renewable Energy and Environmental Laboratories, Via F. Maritano 26, 20097 San Donato Milanese, Italy
[c] Eni S.p.A., Dowstream Process Technology Laboratories, Via F. Maritano 26, 20097 San Donato Milanese, Italy
[d] Università degli Studi di Ferrara, Dipartimento di Scienze Chimiche e Farmaceutiche, Via Fossato di Mortara 17, 44121 Ferrara, Italy

ARTICLE INFO

ABSTRACT

Various civilian, agricultural and industrial activities cause the presence of nitrogen compounds in surface and groundwater, where they are further converted into ammonia and its salts. The progressive increase in ammonium concentration in the environment represents a serious concern since it is one of the main causes of eutrophication and its transformation may lead to carcinogens. On the other hand, wastewater has recently been considered as a potential source of nitrogenous nutrients for plants, once adequate recovery processes have been provided. Among the latter, the adsorption processes must be considered reliable and clean due to the mild operating conditions. An experimental study on the removal of ammonium by adsorption on a zeolite cation exchanger (clinoptilolite mineral) was undertaken, considering the water from an Italian groundwater treatment facility with a treatment capability of 150,000 L/h. The activity was focused on the polishing step before surface discharge (from 20 mg/L to 5 mg/L, according to restrictions due to neighboring water bodies of naturalistic relevance). The experimental study was part of a wider activity for the evaluation of the performances of a 1000 L/h cation-exchange pilot plant operated at the same industrial site. Thus, the peculiar features of the reported study are ammonium removal until the level of traces, use of a conditioned zeolite, and co-presence of high concentrations of other dissolved cationic species competing for exchange.

© 2018 Elsevier Ltd. All rights reserved.

1. Introduction

The presence of nitrogen compounds in surface and groundwater is attributable to several sources including civilian and industrial wastewater, agriculture and animal husbandry. Organic nitrogen is usually converted into ammonium and persists in this form under reducing conditions. Ammonium as such is toxic for fishes (Randall and Tsui, 2002) and is one of the main causes of eutrophication (Smith et al., 1999). Furthermore, changes of chemical conditions or biological processes may lead to its conversion into other compounds, including carcinogenic nitrosamines (Nawrocki and Andrzejewski, 2011).

In recent decades, there has been a progressive increase in concentration of nitrogen compounds in surface and groundwater due to intensive anthropic activities, which has led to serious concerns for water bodies (Ferro, 2012). The improper exercise of such industrial productions, as well as non-sustainable disposal of the resulting waste can have severe impacts on both environment and humans; for instance, the undesired migration of the metals towards other matrices may result in several forms of persistent contamination that would require to be properly quantified (Ferrucci et al., 2017) and dealt with (Vocciante et al., 2017) by referring to specific strategies.

It is always possible to consider at least a cheap and non-invasive control of water movements (Vocciante et al., 2016) — based on inverse strategies already applied on other sectors such as energy recovery (Solisio et al., 2012) — to monitor contaminants

displacement in soil and avoid groundwater contamination by toxic leachate. On the other hand, wastewater can also be considered as a potential source of macronutrients for plants (mainly, nitrogen, phosphorus, potassium) able to front the recent agricultural expansion, once adequate remediation processes have been applied (Xu et al., 2018). Several solutions, including hybrid approaches, have been proposed to achieve ammonium removal from water. The biological approach entails ammonium conversion into nitrate (nitrification) followed by nitrate conversion into nitrogen (denitrification) (Verstraete and Philips, 1998). The physico-chemical approaches include air stripping (Gustin and Marinsek-Logar, 2011), nano-filtration (Marttinen et al., 2002), oxidation (Zhang et al., 2015), precipitation (Doyle and Parsons, 2002), and adsorption (Huang et al., 2018). Specifically, adsorption processes have been recognized as reliable and clean, due to their limited use of chemicals and mild operating conditions (Wang and Peng, 2010). Activated carbon (Vu et al., 2018), hydrogel polymers (Cruz et al., 2018), functionalized polymers (Ancuta et al., 2005) and minerals (Malovanyy et al., 2013) have been proposed as adsorbents for ammonium. In most cases, cation exchange has been identified as the mechanism for ammonium adsorption. Generally, the process takes place with the uptake of one or more cationic species and the simultaneous displacement of an equivalent amount of one or more other cationic species (IUPAC, 2014). Zeolite-based cation exchangers have drawn great attention due to their relevant specific capacity, selectivity, safety and stability in the aggressive environment of wastewater with complex composition (Perego et al., 2013). Their effectiveness has been reported also in the presence of dissolved organic species (Jorgensen, and Weatherley, 2003) and even manure (Wijesinge et al., 2018). Zeolites are crystalline microporous metal silicates (mainly aluminum silicates) with a negatively-charged framework compensated by weakly bounded exchangeable cations (Weitkamp, 2003). Generally, cation exchange equilibrium between a solution containing the cation A^{z_A+} and the B-form of a zeolite (with B as a cation of valence z_B) can be written as reported in Scheme (1) (Perego et al., 2013):

$$z_B A^{z_A^+} + z_A B L z_B \Leftrightarrow z_A B^{z_B^+} + z_B A L z_A \qquad (1)$$

in which L^- is a portion of zeolite framework holding a unit negative charge.

Their use for ammonium removal has been extensively described (Hedstroem, 2001).

Clinoptilolite (with its heulandite framework type, HEU) is one of the most abundant and cheaper zeolite mineral, with $(Me^I,Me^{II}_{0.5})_6[Al_6Si_{30}O_{72}] \times 20H_2O$ (Me^I = Na, K; Me^{II} = Mg, Ca, Sr, Ba) as its idealized chemical formula (Colella, 2005). It is quarried from large natural deposits and considered a mineral commodity quoted about 0.2 USD/kg (to be compared with 1.5 USD/kg of common cation-exchange resins) (Klieve and Semmens, 1980). In addition to cation exchange applications, clinoptilolite has been applied in the manufacturing of building materials, soil modifiers, dietary supplements, dryers, deodorizers and even spacecraft equipment (Mumpton, 1999). The ranking of cation affinity for clinoptilolite reported in Scheme (2) has been widely accepted (Mumpton, 1999), although slight variations have been pointed for different operating conditions or samples (Caputo and Pepe, 2007):

$$Cs^+ > Rb^+ > K^+ > NH_4^+ > Ba^{2+} > Sr^{2+} > Na^+ > Ca^{2+} > Fe^{3+} >$$
$$Al^{3+} > Mg^{2+} > Li^+ \qquad (2)$$
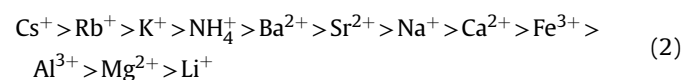
The raw clinoptilolite generally contains huge amounts of potassium that is hard to exchange with ammonium due to its higher affinity. For this reason, exchange with sodium (Weatherley and Miladinovic, 2004) or calcium (Ji et al., 2007) (that is carried out

by repeated washing with concentrated salt solutions) has to be operated before service. The same approach is adopted for regeneration of saturated clinoptilolite within cyclic cation-exchange operations (Hedstroem, 2001). The use of saturated zeolites as soil modifiers has also been proposed, according to a non-regenerative approach (Manto et al., 2018).

Despite the numerous publications on clinoptilolite as ammonium exchanger, comparing the reported results is made difficult by the specificity of the water to be treated, the mineral and the operating procedure (Millar et al., 2016). Furthermore, most published data deal with pristine clinoptilolite, ignoring that the performance at an industrial scale may be different due to its progressive conditioning during service (Klieve and Semmens, 1980).

An experimental study was undertaken, considering a stream from an Italian groundwater treatment facility with a treatment capability of 150,000 L/h (from now on simply defined as "pretreated water") and a clinoptilolite sample taken from a 1000 L/h cation-exchange pilot plant operated at the same industrial site. The activity was focused on the polishing step just before surface discharge, pointing to an ammonium removal until trace level (from 20 mg/L to 5 mg/L). Such ammonium concentration (by far lower than the 15 mg/L limit set by the Italian legislation for surface discharge (Governo Italiano, 2006)) suits restrictions due to nearby water bodies with naturalistic relevance, and represents a novelty with respect to previous investigations.

Presently, the target is obtained by sending the treated water to a water treatment consortium facility. The task is further complicated by the co-presence of high concentrations of other dissolved cationic species, which strongly compete with ammonium for clinoptilolite adsorption, especially at low NH_4^+ contents.

2. Material and methods

2.1. Materials

The pre-treated water (GW) was sampled, stored in polypropylene tanks and kept at 4 °C without any preservative addition. Two different synthetic solutions containing respectively ammonium (S1) and ammonium-and-potassium (S2) were prepared dissolving ammonium chloride and potassium chloride in deionized water. The cation concentrations were adjusted near to the GW ones, in order to evaluate the competition between ammonium and potassium under realistic conditions.

The as received clinoptilolite sample (Me/HEU) underwent washing with deionized water, to remove fine particles and impurities, and sodium exchange to maximize the ammonium specific capacity (Englert and Rubio, 2005). In particular, sodium exchange was carried out according to (Ingleziakis et al., 1999) to obtain the Na/HEU sample, which was then dried at 120 °C for 2400 min in air. Reported data refer to dry sample containing 1% w/w of moisture.

Deionized water with an electrical conductibility of 4 µS/cm was employed. Reagent-grade chemicals were used for solution preparations: ammonium chloride (NH_4Cl, Merck), potassium chloride (KCl, Aldrich), hydrochloric acid (HCl, Carlo Erba), sodium hydroxide (NaOH, Carlo Erba), and sodium chloride (NaCl, Aldrich). Superpure-grade reagents were used for characterization purposes: nitric acid (HNO_3, Carlo Erba), and hydrofluoric acid (HF, Carlo Erba).

2.2. Cation exchange evaluation

The cation-exchange features of Na/HEU were evaluated by kinetic, equilibrium and breakthrough tests, all performed at 20 °C (exploiting the laboratory air conditioning) and atmospheric

pressure.

The kinetic tests were performed by contacting 2.5 g of Na/HEU with 0.5 L of solution (respectively S1 or S2, with a solid/liquid ratio of 5 g/L) adjusted at a pH of 5 to convert the poorly ionized ammonia into ammonium cations (Mazloomi and Jalali, 2016). Several aliquots were sampled at different times, filtered on 0.45 μm cellulose acetate syringe filters (Chromacol) and analyzed. With regard to the tests carried out using GW (after pH adjustment), three kinetic curves were obtained by using solid/liquid ratios of 5, 10 and 20 g/L, respectively.

The equilibrium tests for isotherm curve determination were run using solutions with an ammonium concentration ranging from 10 to 850 mg/L and a potassium content from 10 to 200 mg/L, adopting a solid/liquid ratio of 12.5 g/L. The contact time was set to 240 min according to kinetic results (see below). Both kinetic and equilibrium tests were performed in batch regime, using sealable glass vials under continuous up-down shaking (15 per min) using a Velp Scientifica Rotax 6.8™.

The breakthrough tests were performed using a glass column with an internal diameter of 25 mm and a bed height of 65 mm, filled with 30 g of Na/HEU. The feeding was operated up-flow with a peristaltic pump (Watson Marlow SciQ 400™) and silicone pipes. These tests were performed with S1, S2 and GW, after pH adjustment. Different flow rates were set to evaluate the contact time effect: 0.5, 1 and 2 mL/min, respectively. The Na/HEU bed was changed after each run. Specific ammonium-exchange capacity was evaluated by numerical integration of breakthrough curves.

The regeneration was performed by flushing with a caustic brine made of 1% w/w sodium chloride in deionized water at a pH of 12 (adjusted by sodium hydroxide) in order to convert ammonium into ammonia. A flow rate of 2 mL/min was adopted, stopping the tests when the down-stream concentration of ammonium was close to zero.

The non-linear modelling of experimental data was realized by using the Microsoft Excel 2013 Solver™ package, and setting ordinary least squares (OLS) as the objective function.

2.3. Physico-chemical characterization

The clinoptilolite structural analysis was performed by x-ray powder diffraction (XRD), using a Philips X'Pert™ diffractometer equipped with a pulse-height analyzer and a secondary monochromator. Data were collected in the 2θ angular range from 3° to 50°, with a 0.02° step and 20 s/step accumulation time; the CuKα radiation (wavelength of 1.54178 Å) was used. Qualitative analysis was performed with a search-match method included in the PANalytical X'Pert High Score™ software package.

Alkaline and alkaline-earth metals were quantified by inductively coupled plasma optical emission spectroscopy (ICP-OES) through a Thermo Scientific Icap 6300 Duo™ instrument.

Heavy metals were quantified by inductively coupled plasma mass spectrometry (ICP-MS) by using a Perkin Elmer Elan Drc-e™ instrument.

Clinoptilolite was dissolved with a nitric + hydrofluoric acid mixture in a platinum crucible after drying at 120 °C for 2400 min. All solutions were acidified by adding nitric acid (1% v/v).

Alumina and silica were quantified by x-ray fluorescence spectroscopy (XRF) through a PANalytical Axios Advantage™ instrument on samples vitrified at 1200 °C by a PANalytical Aegon™ oven.

Na/HEU particle size distribution was evaluated by light scattering (Fraunhofer optical model) using a Beckmann Coulter LS13320™ instrument equipped with a Tornado Dry Powder System™.

Ammonium was quantified by ultra-violet visible spectroscopy (UV-VIS) through a Hach Dr5000™ instrument equipped with the Hack Lck303™ kit (indophenol-blue method).

Solution pH and conductivity were measured by a multi-parameter probe Hanna HI7622829™.

Chemical oxygen demand (COD) data were provided by an external laboratory through a standard method (ISPRA, 2003).

All reported data are mean values obtained from experiments performed in duplicate.

3. Results and discussion

The GW sample composition resumed in Table 1 shows the presence of cations potentially competing with ammonium, both in term of selectivity ranking (potassium) and in term of large excess (sodium, calcium, magnesium), in line with Schemes (1) and (2). It is worth noting that the measured COD was less than 80 mg/L (by far lower than the limit of 160 mg/L set by the Italian legislation for surface discharge (Governo Italiano, 2006)) thus any possible interference from organics can be disregarded.

The XRD pattern reported in Fig. 1 refers to Me/HEU; clinoptilolite is confirmed as the main crystalline phase, with minor amounts of quartz and muscovite (the subtended peaks highlight the ideal pattern of clinoptilolite).

The XRD pattern for Na/HEU (not reported) did not show any appreciable variation due to sodium exchange. On the other hand, the data reported in Table 2 confirm the sodium enrichment of the exchanged sample. More than 99% of Na/HEU have a particle size higher than 400 μm with an average of 1200 μm.

The cation-exchange kinetics are reported in Fig. 2; t is the contact time and C the residual concentration of ammonium (or potassium) in solution during experiments carried out with S1 and S2, respectively.

In all cases, the equilibrium was reached within 120 min, with only a slight decrease of the residual concentration of ammonium in solution (C) along an entire day (not reported). In the case of S1, C was equal to 1 mg/L (after 120 min), while it was of 3.5 mg/L in the case of S2 (after 120 min). The situation worsened for the kinetics carried out with GW, as shown in Fig. 3. In this case, C after 120 min was 4.5 mg/L even adopting a solid/liquid ratio of 20 g/L (the quadruple of that used with both S1 and S2).

The equilibrium isotherm curves obtained with synthetic solutions are reported in Fig. 4, where Q_E is the specific amount of exchanged ammonium in equilibrium with C_E.

In particular, Q_E has been estimated according to Equation (3) as the difference between the initial and exchanged ammonium concentrations, C_I and C_E, normalized to the amounts of solution (V) and adsorbing material (M):

$$Q_E = (C_I - C_E)*V/M \tag{3}$$

Regarding S1, the maximum measured exchanged ammonium was of 24 mg/g, which reduced to 10 mg/g in the case of S2. It decreased further down to 4 mg/g in the case of GW, as pointed out in Fig. 5.

Table 1
Main cations dissolved in GW, S1 and S2, respectively.

Specie	Unit	GW	S1	S2
Na^+	mg/L	944	–	–
Ca^{2+}	mg/L	177	–	–
Mg^{2+}	mg/L	89	–	–
K^+	mg/L	41	–	40
NH_4^+	mg/L	17	18	18
Sr^{2+}	mg/L	2	–	–
Fe^{2+}	mg/L	0.75	–	–
Ni^{2+}	mg/L	0.03	–	–

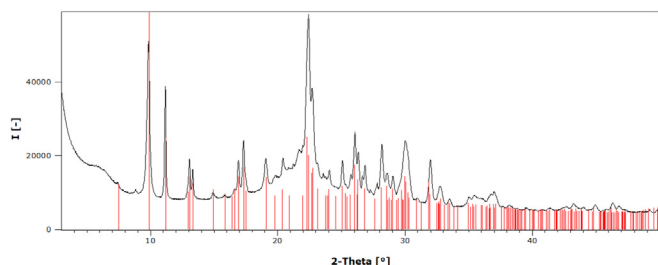**Fig. 1.** XRD pattern of Me/HEU.

Table 2
Chemical compositions of Me/HEU and Na/HEU, respectively.

Specie	Unit	Me/HEU	Na/HEU
SiO_2	% w/w	74	73
Al_2O_3	% w/w	12	12
Na_2O	% w/w	5	7
K_2O	% w/w	4	5
Fe_2O_3	% w/w	3	2
MgO	% w/w	2	1
CaO	% w/w	1	1

The influence of potassium on the equilibrium was quantified by assuming a Langmuir formalism (Foo and Hameed, 2010) for ammonium exchange with S1 and S2, as represented by Equation (5):

$$Q_E = \frac{bC_EQ_M}{1 + bC_E} \tag{5}$$

where Q_E is the exchanged amount of ammonium at equilibrium, Q_M is the limiting exchangeable amount of ammonium, and b is the equilibrium constant. It is worth noting that both Langmuir (Mazloomi and Jalali, 2016) and Freundlich formalisms have been considered adequate for ammonium exchange on clinoptilolite (Millar et al., 2016).

The values of the correlation coefficient (R^2) reported in Table 3 point to the adequacy of experimental data fitting. The reduction of both k and Q_M with S2 are evident; on the other hand, the slight increase of b with S2 is quite surprising and can be interpreted by assuming that the interactions among cation-exchange sites and ammonium are stronger in presence of potassium, even though the availability of exchange sites is limited due to the competition. A deeper interpretation of these macroscopic data, in the absence of further experimental investigations, could be too speculative
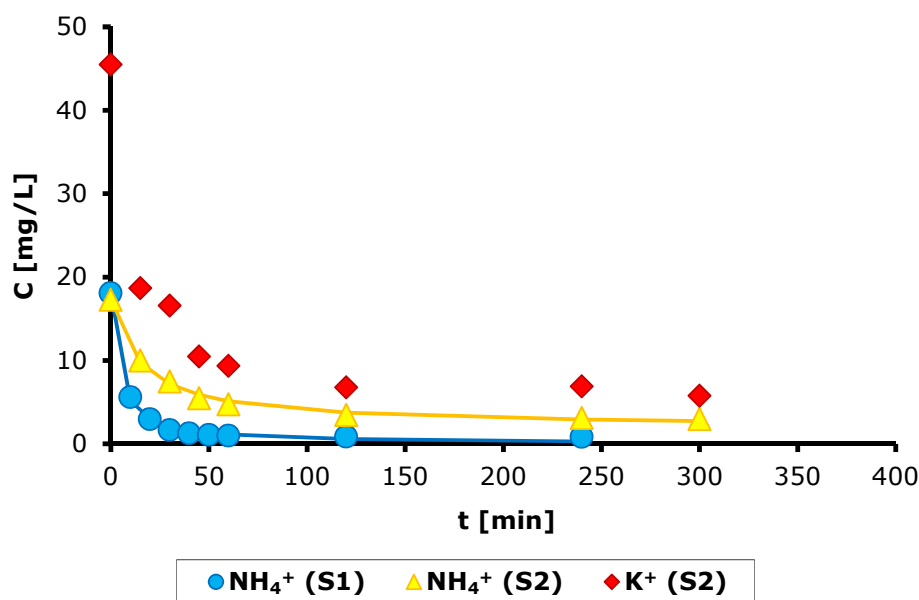

Fig. 2. Cation-exchange kinetics for ammonium and potassium on Na/HEU with S1 and S2, respectively. Dots: experimental data. Lines: pseudo-second order kinetic models.

Both kinetic and equilibrium experiments underlined the competition for the exchange sites among ammonium and other dissolved cationic species.

The influence of potassium on the kinetics was quantified by assuming a pseudo-second order formalism (Gupta and Bhattacharyya, 2011) for ammonium exchange with S1 and S2, according to Mazloomi and Jalali (2016). This is represented by Equation (4):

$$\frac{dQ}{dt} = k(Q_E - Q)^2 \tag{4}$$

where Q_E is the exchanged amount of ammonium at equilibrium, $Q(t)$ is the amount of ammonium exchanged at time t, and k is the pseudo-second order kinetic constant.

(Luetzenkirchen, 1997).

The breakthrough curves obtained by feeding the Na/HEU-packed column with S1 and S2, respectively, are shown in Fig. 6. In this case, C_U and C_D are the up- and down-stream cation concentrations, respectively.

The highest ammonium specific exchange capacity (that corresponds to the highest volume of water that can be fed to the column until Na/HEU saturation) was of 14 mg/g with S1.

Curiously, a C_D/C_U ratio exceeding 1 appeared with S2, possibly justified by an initial accumulation of ammonium on Na/HEU, followed by its progressive displacement due to the incoming potassium. In this case, ammonium specific exchange capacity was of 8 mg/g, while it amounted to 27 mg/g in the case of potassium. As expected, ammonium specific exchange capacity decreased down to 2 mg/g in the case of GW. The flow rate had
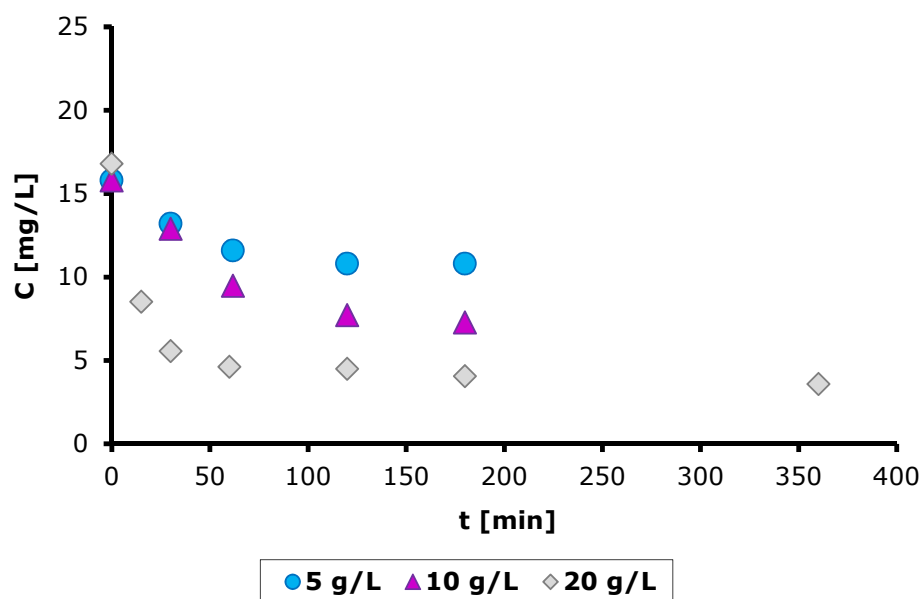
Fig. 3. Cation-exchange kinetics for ammonium on Na/HEU with GW at solid/liquid ratios of 5, 10 and 20 g/L, respectively.
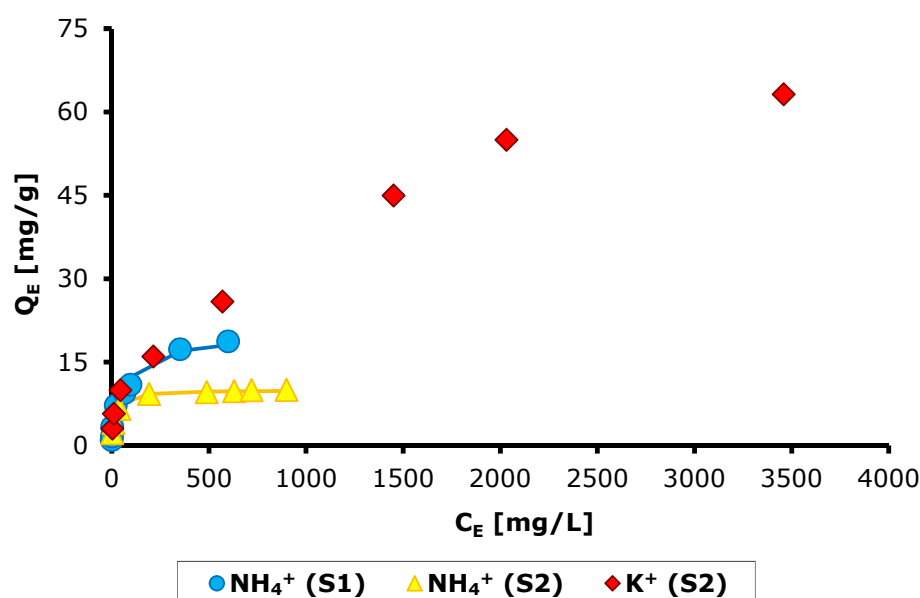

Fig. 4. Cation-exchange isotherms for ammonium and potassium on Na/HEU with S1 and S2, respectively. Dots: experimental data. Lines: pseudo-second order kinetic models.

only a slight influence on the volume of GW supplied before the ammonium concentration exceeded 5 mg/L (corresponding to a C_D/C_U ratio of 0.25). On the other hand, a lower flow rate (which corresponds to a higher contact time) produced a faster saturation of Na/HEU, probably due to a more effective competition among ammonium and other dissolved cations. These evidences are sketched in Fig. 7.

Both a lower specific productivity of fresh water and more frequent regenerations derive from the lower ammonium specific capacity of Na/HEU with GW. Accordingly, the comparison among exchange and regeneration experiments depicted in Figs. 7 and 8, respectively, points that about 20% of fresh water has to be used for the production of brine for regeneration with S1, while it increases to 30% in the case of GW. A huge production of caustic brine is a direct consequence of this.

4. Conclusions

The reported results indicate that ammonium removal from water through cation exchange on clinoptilolite is not a trivial issue in presence of competing cations (especially potassium). In particular, the latter causes both low fresh water specific productivity and frequent regenerations of the adsorbent. Different strategies could be explored to overcome these drawbacks in the context of zeolites:

- the use of synthetic zeolites claimed to be more selective towards ammonium, although more expensive than clinoptilolite (from 1 to over 10 USD/kg (Perego et al., 2013)); in particular, mordenite (Wang et al., 2007), faujasite (Montégut et al., 2016), and ZSM-5 have been proposed (Manto et al., 2018), though the
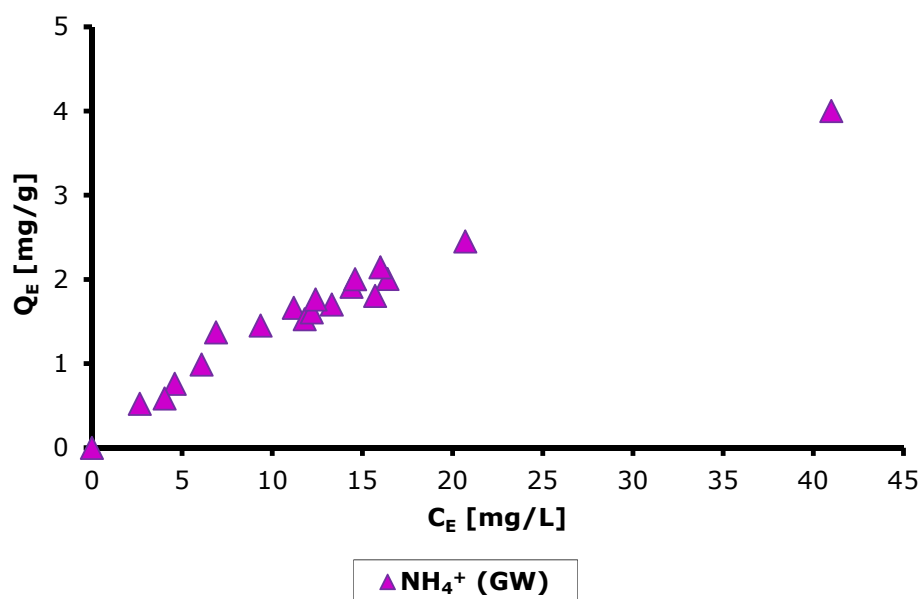
Fig. 5. Cation-exchange isotherm for ammonium on Na/HEU with GW.

Table 3
Cation-exchange kinetics (pseudo-second order) and equilibrium modelling (Langmuir) for ammonium on Na/HEU. Both S1 and S2 solutions are considered.

Parameter	Solution	Unit	Value
Q_E	S1	mg/L	4
k	S1	g/(mg min)	0.07
R^2	S1	–	0.99
Q_E	S2	mg/L	3
k	S2	g/(mg min)	0.02
R^2	S2	–	0.99
Q_M	S1	mg/g	20
b	S1	L/mg	0.02
R^2	S1	–	0.96
Q_M	S2	mg/g	10
b	S2	L/mg	0.07
R^2	S2	–	0.98

operational specificities make experimental trials mandatory (Millar et al., 2016);

- the use of more complex process schemes, including alternative regeneration operations (e.g. biological regeneration) (Hedstroem, 2001);
- the use of a non-regenerative approach, exploiting the saturated clinoptilolite as soil modifier (Leggo et al., 2006).

The optimal choice in designing a remediation process based on this approach will depend on a number of technical and economic factors, to be weighted on a case-by-case basis, but cannot ignore considerations based on the concepts of Circular Economy (European Commission, 2017), BAT techniques, and the "near-zero discharge" of hazardous wastes (see, for example, Pietrelli et al.,
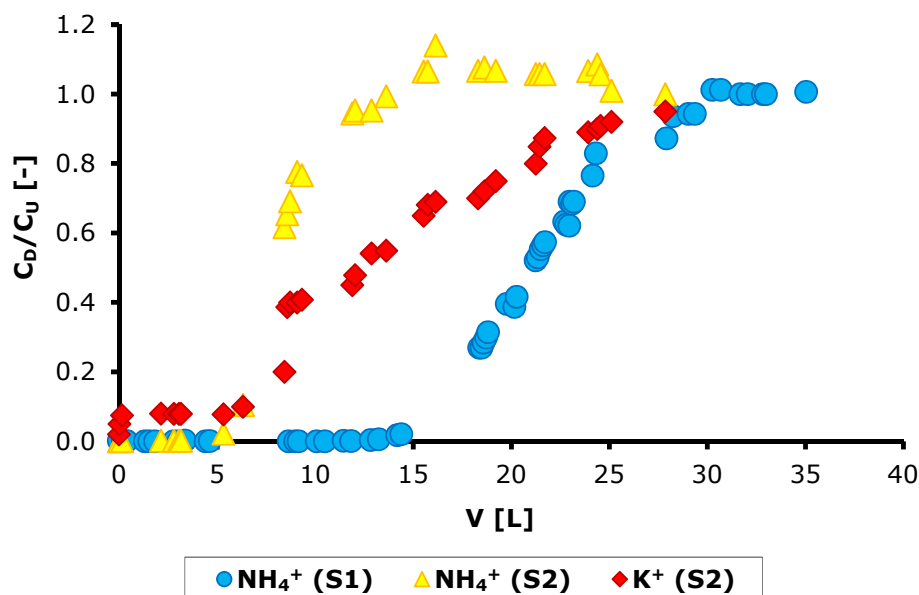

Fig. 6. Breakthrough curves for ammonium and potassium on Na/HEU with S1 and S2, respectively.
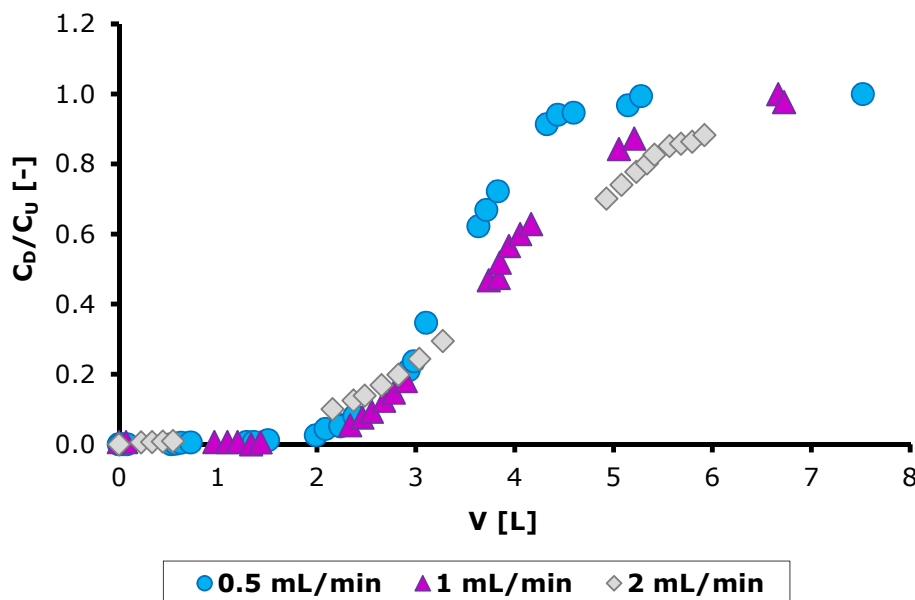
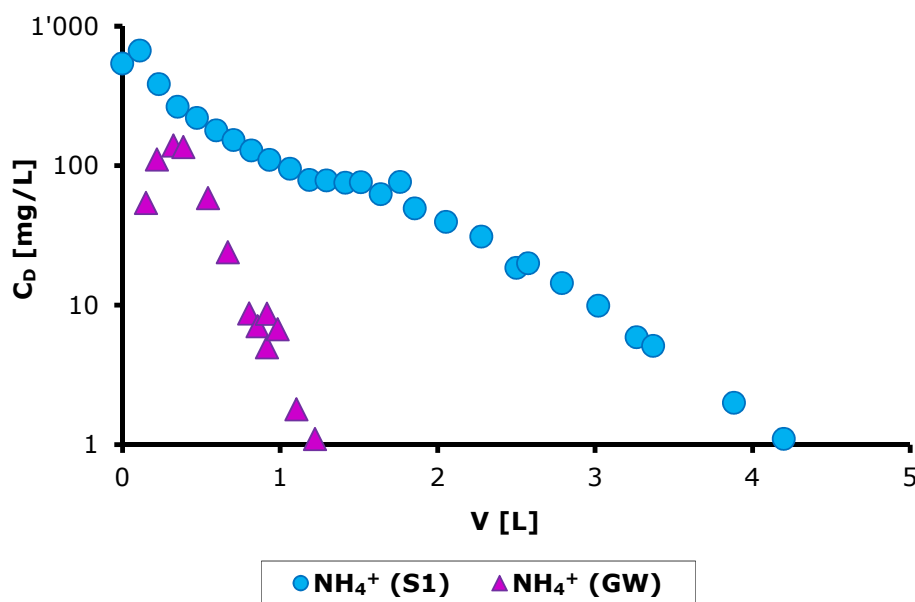**Fig. 7.** Breakthrough curves for ammonium on Na/HEU with GW at flow rates of 0.5, 1 and 2 mL/min, respectively.

Fig. 8. Regeneration curves for Na/HEU saturated with S1 and GW, respectively.

2018), as set by the latest European laws.

Acknowledgments

References

Ancuta, A., Kauspediene, D., Gefeniene, A., Snukiskis, J., Vasileviciute, 2005. Effect of hydroxyl and nitrate ions on the sorption of ammonium ions by sulphonic cation exchangers. Desalination 175, 259–268.

Caputo, D., Pepe, F., 2007. Experiments and data processing of ion exchange equilibria involving Italian natural zeolites: a review. Microporous Mesoporous Mater. 105, 222–231.

Colella, C., 2005. Natural zeolites. Stud. Surf. Sci. Catal. 157, 13–40.

Cruz, H., Luckman, P., Seviour, T., Verstraete, W., Laicock, B., Pikaar, I., 2018. Rapid removal of ammonium from domestic wastewater using polymer hydrogels. Sci. Rep. 8, 1–6.

Doyle, J.D., Parsons, S.A., 2002. Struvite formation, control and recovery. Water Res. 36, 3925–3940.

Englert, A.H., Rubio, J., 2005. Characterisation an environmental application of a Chilean natural zeolite. Int. J. Miner. Process. 75, 21–29.

EC, 2017. Report from the Commission to the European Parliament, the Council, the European Economic and Social Committee and the Committee of the Regions on the Implementation of the Circular Economy Action Plan, Version 371 Bruxelles 26/01/2017. COMM 33 Final. European Commission, Bruxelles, Belgium. ec.europa.eu/environment/circular economy/implementation_report_annex.pdf. (Accessed 18 June 2018).

Ferro, S., 2012. Removal of nitrates from highly-contaminated industrial waste-water. Chim. Ind. 94 (3), 100–110.

Ferrucci, A., Vocciante, M., Bagatin, R., Ferro, S., 2017. Electrokinetic remediation of soils contaminated by potentially toxic metals: dedicated analytical tools for assessing the contamination baseline in a complex scenario. J. Environ. Manag. 203, 1163–1168.

Foo, K.Y., Hameed, B.H., 2010. Insights into the modeling of adsorption isotherm

systems. Chem. Eng. J. 156, 2—10.

Governo Italiano, 2006. Emission Limit Values in Surface Water and in Drainage. Legislative Decree 152/2006, Part 3, Annex 5, Table 3 (Governo Italiano, Roma, Italy).

Gupta, S.S., Bhattacharyya, K.G., 2011. Kinetics of adsorption of metal ions on inorganic materials: a review. Adv. Colloid Interface Sci. 162, 39—58.

Gustin, S., Marinsek-Logar, R., 2011. Effect of pH, temperature and air flow rate on the continuous ammonia stripping of the anaerobic digestion effluent. Process Saf. Environ. Protect. 89, 61—66.

Hedstroem, N., 2001. Ion exchange of ammonium on zeolites: a literature review. J. Environ. Eng. 127 (8), 673—681.

Huang, J., Kankanamge, N.R., Chour, C., Welsh, D.T., Li, T., Teasdale, P.R., 2018. Removing ammonium from water and wastewatere using cost-effective adsorbents: a review. J. Inst. Environ. Sci. 63, 174—197.

Ingleziakis, V.J., Diamandis, N.A., Loizidou, M.D., Grigoropolulou, H.J., 1999. Colloid Interface Sci. 215, 54—57.

ISPRA, 2003. Istituto Superiore per la Protezione e la Ricerca Ambientale, APAT CNR IRSA 2060 Manual 29. Istituto Superiore per la Protezione e la Ricerca Ambientale, Roma, Italia. www.isprambiente.gov.it/it/pubblicazioni/manuali-e-linee-guida/metodi-analitici-per-le-acque (accessed 20 September 2017).

IUPAC, 2014. International Union of Pure and Applied Chemistry, Compendium of Chemical Terminology, Gold Book, Version 2.3.3. International Union of Pure and Applied Chemistry, Zurich, Switzerland (accessed 19 June 2017). goldbook. iupac.org/pdf/goldbook.pdf.

Jorgensen, T.C., Weatherley, L.R., 2003. Ammonia removal from wastewater by ion exchange in the presence of organic contaminants. Water Res. 37, 1723—1728.

Ji, Z.Y., Yuan, J.S., Li, X.G., 2007. Removal of ammonium from wastewater using calcium form clinoptilolite. J. Hazard. Mater. 141 (3), 483—488.

Klieve, J.R., Semmens, M.J., 1980. An evaluation of pretreated natural zeolites for ammonium removal. Water Res. 14, 161—168.

Leggo, P.J., Ledesert, B., Christie, G., 2006. The role of clinoptilolite in organo zeolitic soil systems used for phytoremediation. Sci. Total Environ. 363, 1—10.

Luetzenkirchen, J., 1997. Ionic strength effects on cation sorption to oxides: macroscopic observations and their significance in microscopic interpretation. J. Colloid Interface Sci. 195, 149—155.

Malovanyy, A., Sakalova, H., Yatchyshyn, Y., Plaza, E., Malovanyy, M., 2013. Concentration of ammonium from municipal wastewater using ion exchange process. Desalination 329, 93—102.

Manto, M.J., Xie, P., Keller, M.A., Liano, W.E., Pu, T., Wang, C., 2018. Recovery of ammonium from aqueous solutions using ZSM-5. Chemosphere 198, 501—509.

Marttinen, S.K., Kettunen, R.H., Sormunen, K.M., Soimasuo, R.M., Rintala, J.A., 2002. Screening of physical—chemical methods for removal of organic material, nitrogen and toxicity from low strength landfill leachates. Chemosphere 46, 851—858.

Mazloomi, F., Jalali, M., 2016. Ammonium removal from aqueous solutions by natural Iranian zeolite in the presence of organic acids, cations and anions. J. Environ. Chem. Eng. 4, 240—249.

Millar, G.J., Winnett, A., Thompson, T., Couperthwaite, S.J., 2016. Equilibrium studies of ammonium exchange with Australian natural zeolites. J. Water Proc. Eng. 9,

47—57.

Montégut, G., Michelin, L., Brendlé, J., Lebeau, B., Patarin, J., 2016. Ammonium and potassium removal from swine liquid manure using clinoptilolite, chabazite and faujasite zeolite. J. Environ. Manag. 167, 147—155.

Mumpton, F.A., 1999. La roca magica: uses of natural zeolites in agriculture and industry. Proc. Nat. Acad. Sci. USA 96, 3463—3470.

Nawrocki, J., Andrzejewski, P., 2011. Nitrosamines and water. J. Hazard Mater. 189, 1—18.

Perego, C., Bagatin, R., Tagliabue, M., Vignola, R., 2013. Zeolites and related mesoporous materials for multi-talented environmental solutions. Microporous Mesoporous Mater. 166, 37—49.

Pietrelli, L., Ferro, S., Vocciante, M., 2018. Raw materials recovery from spent hydrochloric acid-based galvanizing wastewater. Chem. Eng. J. 341, 539—546.

Randall, D.J., Tsui, T.K.N., 2002. Ammonia toxicity in fish. Mar. Pollut. Bull. 45, 17—23.

Smith, V.H., Tilman, G.D., Nekola, J.C., 1999. Eutrophication: impacts of excess nutrient inputs on freshwater, marine, and terrestrial ecosystems. Environ. Pollut. 100, 179—196.

Solisio, C., Reverberi, A.P., Del Borghi, A., Dovì, V.G., 2012. Inverse estimation of temperature profiles in landfills using heat recovery fluids measurements. J. Appl. Math. 2012, 747410.

Verstraete, W., Philips, S., 1998. Nitrification-denitrification processes and technologies in new contexts. Environ. Pollut. 102 (SI), 717—726.

Vocciante, M., Reverberi, A.P., Dovì, V.G., 2016. Approximate solution of the inverse Richards' problem. Appl. Math. Model. 40, 5364—5376.

Vocciante, M., Bagatin, R., Ferro, S., 2017. Enhancements in electrokinetic remediation technology: focus on water management and wastewater recovery. Chem. Eng. J. 309, 708—716.

Vu, M.T., Chao, H.P., Trinh, T.V., Trinh, T.L., Lin, C.C., Tran, H.N., 2018. Removal of ammonium from ground water using NaOH treasted activated carbon derived from corncob wastes: batch and column experiments. J. Clean. Prod. 180, 560—570.

Wang, Y., Kmiya, Y., Okuhara, T., 2007. Removal of low concentration ammonia in water by ion exchange using sodium mordenite. Water Res. 41, 269—276.

Wang, S., Peng, Y., 2010. Natural zeolites as effective adsorbents in water and wastewater treatment. Chem. Eng. J. 156, 11—24.

Weatherley, L.R., Miladinovic, N.D., 2004. Comparison of the ion exchange uptake of ammonium ion onto New Zealand clinoptilolite and mordenite. Water Res. 38, 4305—4312.

Weitkamp, J., 2003. Zeolites and catalysis. Solid State Ionics 52, 989—995.

Wijesinge, D.T.N., Dassanayake, K.B., Scales, P.J., Sommer, S.G., Chen, D., 2018. Effect of Australian zeolite on methane production and ammonium removal during anaerobic digestion of swine manure. J. Environ. Chem. Eng. 6, 1233—1241.

Xu, K., Lin, F., Dou, X., Zeng, M., Tan, W., Wang, C., 2018. Recovery of ammonium and phosphate from urine as value-added fertilizer using wood waste biochar loaded with magnesium oxides. J. Clean. Prod. 187, 205—214.

Zhang, X., Li, W., Blatchley III, E.R., Wang, X., Ren, P., 2015. UV-chlorine process for ammonia removal and disinfection by-product reduction: comparison with chlorination. Water Res. 68, 804—811.